

RSC Advances



This is an *Accepted Manuscript*, which has been through the Royal Society of Chemistry peer review process and has been accepted for publication.

Accepted Manuscripts are published online shortly after acceptance, before technical editing, formatting and proof reading. Using this free service, authors can make their results available to the community, in citable form, before we publish the edited article. This *Accepted Manuscript* will be replaced by the edited, formatted and paginated article as soon as this is available.

You can find more information about *Accepted Manuscripts* in the [Information for Authors](#).

Please note that technical editing may introduce minor changes to the text and/or graphics, which may alter content. The journal's standard [Terms & Conditions](#) and the [Ethical guidelines](#) still apply. In no event shall the Royal Society of Chemistry be held responsible for any errors or omissions in this *Accepted Manuscript* or any consequences arising from the use of any information it contains.

Cite this: DOI: 10.1039/c0xx00000x

www.rsc.org/xxxxxx

ARTICLE TYPE

Composite electrode of TiO₂ particles with different crystal phases and morphology to significantly improve the performance of dye-sensitized solar cells

Jinglei Xu, Jingpeng Jin, Zihao Ying, Wenye Shi, and Tianyou Peng*

5 Received (in XXX, XXX) Xth XXXXXXXXXX 20XX, Accepted Xth XXXXXXXXXX 20XX

DOI: 10.1039/b000000x

A novel composite electrode containing brookite TiO₂ quasi nanocubes and anatase TiO₂ sea urchin-like microspheres is fabricated for improving the dye-sensitized solar cell's performance. The brookite nanocubes have a mean size of ~50 nm, and the anatase microspheres with ~3 μm diameter display hierarchical structures composed of secondary TiO₂ nanoribbons and nanoparticles. An optimal efficiency of 7.09% is obtained from the solar cell fabricated with a composite TiO₂ electrode containing 30wt% nanocubes and 70wt% microspheres, with 81% or 30% improvement in the efficiency as compared to the single nanocubes or microspheres film-based cell. Those brookite nanocubes in the microsphere film can fill into the interspaces of the hierarchical microspheres, which can not only enhance the dye-loading, but also reduce the charge recombination. All these lead to the higher voltage and current, and then causing the improved performance of the anatase TiO₂ film-based solar cell.

1 Introduction

Dye-sensitized solar cells (DSSCs) have promoted the intense researches in the past decades since the pioneering work on the photoelectric conversion efficiency of 7% by using nanocrystal TiO₂ porous film electrode was reported in 1991.¹ Compared to the conventional silicon-based photovoltaic devices, DSSCs hold the promise of lower fabrication cost and have efficiency comparable to the amorphous silicon solar cells.^{2,3} Recently, perovskite solar cells are emerging as highly efficient photoelectric conversion devices with efficiency of >19%.⁴ Nevertheless, perovskite solar cells suffer from the lack of thermal stability and their power conversion efficiency is significantly affected by the ambient humidity. Although the record conversion efficiency (~12%) is much lower than that of the perovskite solar cells,³ the TiO₂ film based DSSCs are relatively environmentally stable with more flexible designs and more eco-friendly features, which might be beneficial for promoting the practical application of those DSSCs.¹⁻³

Among the three TiO₂ crystallographic forms that exist in nature, anatase, rutile or their mixed crystal, have been extensively investigated and widely applied in the fields of photocatalysis and solar cells,¹⁻⁷ while the thermodynamically instable brookite is rarely studied due to the difficulty encountered in obtaining its pure phase.⁸⁻¹⁰ For many years, the majority of

attempts for the pure brookite TiO₂ only obtained mixed crystal containing a secondary phase such as anatase and/or rutile. For example, TiO₂ nanorods with brookite/anatase/rutile mixed crystal were synthesized from tetrabutyl-titanate in an acidic condition by using toluene substance.⁸ Moreover, only brookite/anatase mixed crystals were obtained by using titanium bis(ammoniumlactate) dihydroxide as Ti source though the brookite/anatase ratio can be tuned *via* changing the urea concentration, and it was found that those products containing brookite showed significantly high conversion efficiency in photo-oxidization of CH₃OH to HCHO.⁹ In 2009, a kind of flower-like brookite TiO₂ particles with high phase purity were synthesized by optimizing the Na⁺ and OH⁻ concentrations in a reaction system, and the obtained brookite showed a direct transition with a band-gap of 3.4 eV, which is obviously larger than those of the other polymorphs, that is, an indirect bandgap of 3.2 eV for anatase and a direct bandgap of 3.0 eV for rutile.¹¹ Subsequently, single-crystal brookite TiO₂ nanosheets with exposed specific facets were also synthesized by a similar method,¹² which offered a strategy for tuning catalysts from being inert to having high photoreduction reactivity through tailoring of the morphology and surface structure.¹²

It was reported that the bandgap energy (E_g) of the TiO₂ polymorphs is in the sequence of $E_{g, \text{brookite}} > E_{g, \text{anatase}} > E_{g, \text{rutile}}$.¹³ Since the three crystal phases have a similar valence band (VB) level due to their identical elementary composition, brookite TiO₂ should exhibit the most negative conduction band (CB) level among the three polymorphs, and then contribute a higher open-circuit voltage (V_{oc}) as photoanode material in DSSCs than anatase and rutile.⁵⁻⁷ This conjecture is validated by the previous results on the brookite TiO₂-based cells, which usually exhibited

College of Chemistry and Molecular Science, Wuhan University, Wuhan 430072, P. R. China. E-mail: typeng@whu.edu.cn; Fax: 86 27 68752237.

higher V_{oc} than the anatase TiO_2 -based ones.¹⁴⁻¹⁷ Nevertheless, a record efficiency of those single brookite TiO_2 film-based solar cells is only 5.97% until now,^{14,15} which is much lower than that of those anatase TiO_2 film-based ones. Therefore, it is still necessary to exploit some new routes to take advantage of the most negative CB of the brookite TiO_2 so as to further improve the photovoltaic performance of the DSSCs.

In 2002, the first DSSC using a composite TiO_2 electrode containing 75% brookite and 25% anatase showed an impressively improvement in the performance of DSSCs.¹⁸ More recently, thermally stable brookite TiO_2 with single phase and rice-like morphology was prepared through a hydrothermal method,¹⁹ and its average diameter (brachyaxis of the rice-like particle) can be widely tuned in the range of 200-1200 nm by varying the reaction condition, and those rice-like brookite TiO_2 particles with high phase purity and ~600 nm particle diameter as overlayer of an nanosized anatase TiO_2 -based film can improve the photovoltage and efficiency of the nanosized TiO_2 -based solar cells.^{19,20} The above results gave us inspiration that significant enhancement in the conversion efficiency may be realized once the anatase TiO_2 combines with brookite TiO_2 . To the best of our knowledge, there is few investigation focused on the anatase/brookite TiO_2 composite electrode for improving the photovoltaic performance of the DSSCs.¹⁸

Recently, anatase TiO_2 sea urchin-like microspheres with ~3 μm diameter were synthesized via a one-step solvothermal method by using titanium tetrabutoxide as Ti source in our group.²¹ The TiO_2 microspheres display hierarchical structures containing secondary TiO_2 nanoribbons and nanoparticles with an average particle size of ~15 nm. It was found that this anatase TiO_2 hierarchical microspheres as photoanode material of a quasi-solid-state plastic-based flexible solar cells can not only enhance the dye loading, but also strengthen the particle interconnections of the film electrode derived from a low-temperature preparation process, which leads to a lower charge recombination, and hence a better efficiency (4.32%) compared to the nanosized TiO_2 film-based one (2.21%).²¹ The above features such as large sphere diameter and specific surface area, urchin-like hierarchical structure imply that some brookite TiO_2 nanoparticles with small size can be embedded in the interstices of the microspheres to form intimate contacts between the anatase and brookite TiO_2 , which is a benefit to significantly enhance the charge separation and then the conversion efficiency of the DSSCs. To efficiently combine with those microspheres, thermally stable brookite TiO_2 quasi nanocubes with high phase purity and much smaller sizes (~50 nm) are synthesized through a hydrothermal method by using $TiCl_4$ as Ti source, and then the above brookite nanocubes and anatase microspheres are used to prepare the composite TiO_2 photoanode for DSSCs. An optimal power conversion efficiency of 7.09% is obtained from a solar cell fabricated with a composite TiO_2 electrode containing 30wt% brookite nanocubes and 70wt% anatase microspheres, with 81% or 30% improvement in the conversion efficiency as compared to the single brookite TiO_2 nanocubes or anatase TiO_2 microspheres film-based solar cell, respectively. The functioning of the composite electrode containing different crystal phases and morphology is thoroughly investigated by using electrochemical and photoelectrochemical measurement techniques.

2 Experimental section

2.1 Material preparation and characterization

All reagents are of analytical grade and used as received without further purification. A typical preparation process of the brookite TiO_2 nanocubes is as follows: A fixed amount of $TiCl_4$ was added drop by drop to a Teflon autoclave containing 40 mL deionized water cooled by an ice-water bath, and then 2.0 g urea was mixed and dissolved in this solution with agitation. After that, 2.0 mL of sodium lactate liquor (60%) was dropped in the mixed solution while stirring for 30 min. The clarified liquid obtained was then subjected to hydrothermal treatment at 200°C for 20 h. After that, the white precipitate was separated by centrifugation (4000 rpm), and then washed several times with distilled water and absolute ethanol, dried at 70°C in air. Finally, the as-prepared product was further calcined at 500°C for 3 h with a heating rate of 2°C min⁻¹.

The anatase TiO_2 hierarchical microspheres are prepared *via* a facile one-step solvothermal method according to our previous report.²¹ Typically, 4 mL of titanium tetrabutoxide (TBOT) was dispersed in 120 mL acetic acid. After stirring for 10 min, the solution was sealed in a Teflon lined stainless steel autoclave (160 mL) and heated at 140°C for 72 h. After cooled to room temperature naturally, the product was separate by centrifugation (4000 rpm), and washed several times with distilled water and absolute ethanol, and then dried at 70°C in air. Finally, the product was further calcined at 500°C for 3 h.

Phase analyses with X-ray diffraction (XRD) method were performed on a D8-advance X-ray diffractometer (Bruker) with Cu K α radiation ($\lambda=0.15418$ nm). A scan rate of 2° min⁻¹ was applied to record the XRD patterns in the range of $2\theta=20^\circ-50^\circ$. The microstructures were explored by a high-resolution transmission electron microscope (HRTEM, JEM 2100F). The morphology was investigated by scanning electron microscope (SEM, JSM-6700F). Nitrogen adsorption-desorption isotherms at 77 K were measured on a Micrometrics ASAP 2010 system after samples were degassed at 120 °C. UV-vis diffuse reflectance absorption spectra (DRS) were obtained with a UV-vis-NIR spectrophotometer (Shimadzu UV-3600) equipped with an integrating sphere with BaSO₄ as the reference.

2.2 Photoanodes preparation and solar cell fabrication

A typical photoanode preparation process is as follows: A 1.0 g portion of TiO_2 containing different weight ratios of the obtained brookite nanocubes/anatase microspheres was mixed with 8.0 mL of ethanol, 0.2 mL of acetic acid, 3.0 g of terpinol and 0.5 g of ethyl cellulose by ball-milling for 10 h. The obtained paste was spread on a clean FTO glass (15 Ω sq⁻¹) by using the doctor blading technique. The thicknesses of the films were controlled by adhesive tape (Scotch, 50 μm) serving as spacer. After drying in atmosphere, the film was sintered at 500°C for 30 min to remove the binders in the paste.

Dye sensitization was achieved by soaking the electrodes into a 0.3 mM N719 dye (Solaronix) in ethanol solution for 20 h, followed by rinsing in ethanol and drying in air. The dye-sensitized electrode was assembled in a typical sandwich-type cell. A Pt-coated FTO counter electrode was placed over the dye-sensitized electrode. The electrolyte which consists of 0.5 M LiI, 0.05 M I₂ and 0.1 M 4-*tert*-butylpyridine in 1:1 acetonitrile-

propylene carbonate was injected into the interspace between the electrodes to fabricate the solar cell.

In order to describe conveniently, the solar cell fabricated with single brookite TiO₂ nanocubes or anatase TiO₂ microspheres TiO₂ film-based photoanode was denoted as 100B and 100A, respectively. Similarly, the solar cell fabricated with the composite TiO₂ electrode was denoted as xByA, where x represents x wt% brookite nanocubes (B) and y wt% anatase microspheres (A) used for the preparation of the composite electrode. For instance, 30B70A means the solar cell is fabricated with a composite TiO₂ electrode containing 30wt% brookite nanocubes and 70wt% anatase microspheres.

2.3 Solar cell performance measurement

The solar cell was illuminated by light with energy of 100 mW cm⁻² (AM1.5G) from a 300 W solar simulator (Newport, 91160). The light intensity was determined using a reference monocrystalline silicon cell system (Oriel, U. S. A). Computer-controlled Keithley 2400 sourcemeter was employed to collect the photocurrent-voltage (*J-V*) curves of DSSCs. The active area was 0.16 cm². To estimate the dye-adsorbed amount of TiO₂ films, the dyed film electrode was separately immersed into a 0.1 M NaOH solution in a mixed solvent (*V*_{water}: *V*_{ethanol}=1:1), which resulted in desorption of N719 dye molecules. The absorbance of the resultant solution was measured by a UV-3600 UV-vis spectrophotometer (Shimadzu, Japan). The dye-adsorbed amount was determined by the molar extinction coefficient of 1.41 × 10⁴ dm³ mol⁻¹ cm⁻¹ at 515 nm as reported previously.²¹

Electrochemical impedance spectroscopy (EIS) was obtained by applying bias of the open-circuit voltage without electric current under 100 mW cm⁻² illumination and were recorded over a frequency range of 0.05-10⁵ Hz with ac amplitude of 10 mV. For the open-circuit voltage decay (OCVD) measurement, the illumination was turned off using a shutter after the cell was first illuminated to a steady voltage, and then the OCVD curve was recorded. The above photoelectrochemical measurements were carried out on a CHI-604C electrochemical analyzer.

3 Results and discussion

3.1 Crystal phase and microstructure analyses

Fig. 1 depicts the XRD patterns of the obtained brookite TiO₂ nanocubes and anatase TiO₂ microspheres. As shown in Fig. 1a, the product derived from the hydrothermal treatment of TiCl₄ solution followed by calcination at 500°C for 3h shows an orthorhombic brookite phase (JCPDS 65-2448).^{19,20,22} The diffraction peaks at 2θ=25.3, 25.7, 30.8, 32.9, 36.2, 37.3, 40.1, 42.4, 46.0, 48.0, and 49.1° can be attributed to the reflection of (210), (111), (211), (020), (102), (021), (202), (221), (302), (321), and (312) planes, respectively. No diffraction peak for any other TiO₂ crystal phase can be observed, indicating this product has high crystallinity and phase purity, which is in well agreement with our previous works.^{19,20} Although it is a common sense that brookite TiO₂ is a thermodynamically instable phase, the present product still maintains the brookite phase even after calcination at 500°C, confirming its good thermal stability. Since the electrode should be fabricated through sintering at 500°C to remove the binders in the electrode paste, it can be concluded that this

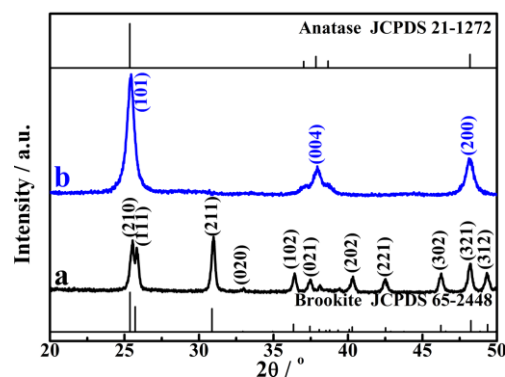


Fig.1 XRD patterns of the obtained brookite TiO₂ nanocubes (a) and anatase TiO₂ sea urchin-like microspheres (b).

product could remain its brookite phase during the electrode fabrication process. Fig. 1b shows the XRD pattern of the product derived from the solvothermal treatment of titanium tetrabutoxide solution followed by calcination at 500°C. The diffraction peaks at 2θ=25.2, 37.8, and 48.1° in the XRD pattern are identified to a pure anatase TiO₂ (JCPDS 21-1272), and attributed to the diffraction of (101), (004), and (200) planes,²¹ respectively.

Fig. 2 shows the SEM and TEM images of the obtained brookite TiO₂ nanocubes and the anatase TiO₂ microspheres. As can be seen from Fig. 2a, the brookite TiO₂ shows a significant proportion of TiO₂ particles with quasi nanocube-like morphology. Those brookite TiO₂ quasi nanocubes with smooth surface and sharp corners have relative uniform particle sizes in the range of 20-75 nm with a mean particle size of ~50 nm. This observation can be further validated by the TEM image shown in Fig. 2b. Those quasi nanocubes with an average diameter of ~50 nm also show uniform and discrete perspective projections with relatively smooth surfaces and sharp edges similar to the observation from the above SEM image, indicating the quasi nanocubes are a complete particle but not an aggregate of small primary nanoparticles. Moreover, the HRTEM image (inset in Fig. 2b) indicates that the lattice spacing is ~0.351 nm, which is consistent with the (210) planes of the brookite TiO₂, and the (111) lattice fringes with d-spacing of ~0.346 nm can also be clearly observed, which corresponds to the strongest diffraction peak of (111) planes shown in the XRD pattern (Fig. 1). The crystal face angle of the two crystal planes is ~79.8°, which is consistent with the theoretical value.^{19,20} Furthermore, the clear lattice fringes reveal the single-crystal characteristics and high crystallinity of the present brookite TiO₂ nanocubes.

SEM image (Fig. 2c) illustrates that the obtained anatase TiO₂ product consists of well-defined sea urchin-like microspheres composed of hierarchical TiO₂ nanoparticles and nanoribbons, which is consistent with our previous report on the preparation of the urchin-like microspheres with relative uniform diameters (~3 μm).²¹ TEM image (Fig. 2d) shows the sea urchin-like microsphere is composed of nanoparticles and nanoribbons, while the nanoribbons show a hierarchical structure composed of small secondary nanoparticles. The HRTEM image (inset in Fig. 2d) of the microsphere also shows clear lattice fringes with an interplanar spacing of ~0.352 nm, corresponding to the d-spacing of the anatase (101) planes. The clear lattice fringes reveal the single-crystal feature and high crystallinity of the anatase microspheres. Generally speaking, these sea urchin-like micro-

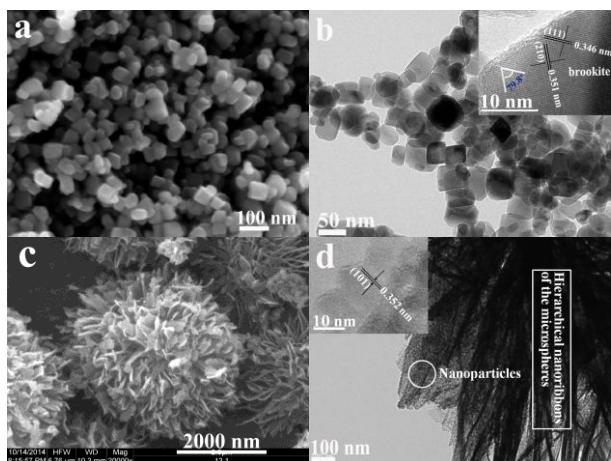


Fig. 2 SEM (a, c) and TEM (b, d) images of the obtained brookite TiO₂ nanocubes (a, b) and anatase TiO₂ sea urchin-like microspheres (c, d).

spheres have hierarchical structures composed of anatase TiO₂ nanoribbons, which are primarily made up of secondary nanoparticles with average particle size of ~15 nm.²¹

Fig. 3 shows the nitrogen adsorption-desorption isotherms and the corresponding Barret-Joyner-Halenda (BJH) pore size distribution plots (inset) of the obtained brookite TiO₂ nanocubes and anatase TiO₂ microspheres. As can be seen, the brookite TiO₂ nanocubes display a typical type III isotherm with H3 hysteresis loops. The condensation of N₂ among those inter-crystallite pores stemmed from those stacked particles brings about a jump in the N₂ adsorption branches starting at a very high relative pressure region ($P/P_0 = 0.82$) with the Brunauer-Emmett-Teller (BET) specific surface area of ~34.2 m² g⁻¹, and its broad BJH pore size distribution plot determined from the desorption branches is in the range of 10-100 nm centered at 30 nm, corresponding to the intercrystal voids among those stacked nanocubes. The anatase TiO₂ microspheres show a type IV isotherm, which is usually attributed to the predominance of mesoporous structure.²¹ The BJH pore size distribution of the anatase microspheres is broader than that of the brookite nanocubes, but the BJH plot mainly contains mesopores with ~10 nm pore width. It can be attributed to the inner mesopores of the hierarchical ribbons and nanoparticles, which contributes a much larger specific surface area (~74.8 m² g⁻¹) than that (~34.2 m² g⁻¹) of the brookite nanocubes.

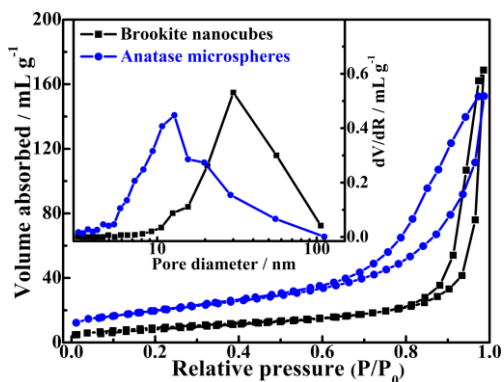


Fig. 3 N₂ adsorption-desorption isotherm and BJH pore size distribution plots (inset) of the brookite TiO₂ nanocubes and anatase TiO₂ microspheres.

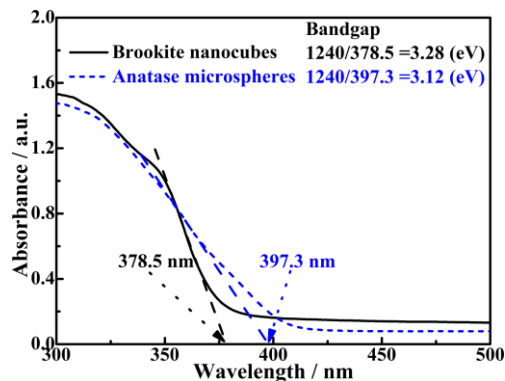


Fig. 4 UV-vis diffuse reflectance absorption spectra (DRS) of the obtained brookite TiO₂ nanocubes and anatase TiO₂ microspheres.

Fig. 4 shows the UV-vis diffuse reflectance absorption spectra (DRS) of the brookite TiO₂ nanocubes and the anatase TiO₂ microspheres. As shown in Fig. 4, the bandgap energy (E_g) of the brookite nanocubes and the anatase microspheres can be estimated to be 3.28 and 3.12 eV according to their absorption band edges at 378.5 and 397.3 nm, respectively. The bandgap energy of the brookite TiO₂ is 0.16 eV higher than the anatase TiO₂, which is consistent with the previous investigation.¹¹ Since the same elementary composition of brookite and anatase TiO₂ means an identical VB level,⁵⁻⁷ it can be concluded that the brookite TiO₂ nanocubes as photoanode material would have a higher Fermi level, and then a higher open-circuit voltage (V_{oc}) in DSSCs than the anatase TiO₂ microspheres, which will be discussed in the following section.

3.2 Photovoltaic performance analyses of the solar cells

The single brookite TiO₂ nanocubes or anatase TiO₂ microspheres film-based solar cells are firstly fabricated and illuminated by simulated AM1.5G solar light with energy of 100 mW cm⁻² for the photovoltaic performance measurements. Fig. 5 depicts the J - V curves of those solar cells, and their corresponding short-circuit current densities (J_{sc}), open-circuit photovoltage (V_{oc}), fill factors (FF), and overall conversion efficiencies (η) are summarized in Table 1. As can be seen, the brookite TiO₂ nanocubes film-based cell (100B) yields a 3.92% efficiency with J_{sc} =7.38 mA cm⁻², V_{oc} =0.73 V, and FF=0.73, whereas the anatase TiO₂ microspheres film-based one (100A) shows 5.47% efficiency with J_{sc} =12.63 mA cm⁻², V_{oc} =0.65 V, and FF=0.67. Namely, the brookite nanocubes as photoanode material of DSSCs displays a higher V_{oc} than the anatase TiO₂ microspheres, which is may be related to the higher CB level of the brookite as compared to anatase.²³ Moreover, it has been reported that the higher V_{oc} of the brookite TiO₂ film-based solar cell than the anatase TiO₂ film-based one is due to the lower reactivity of the brookite surface, which causing a reduced charge recombination.¹⁶ Therefore, it can be concluded that the higher V_{oc} of the brookite TiO₂ nanocubes as photoanode material can be attributed to the higher Fermi level and lower surface reactivity as compared to the anatase microspheres.

Nevertheless, the efficiency (3.92%) of the brookite TiO₂ nanocubes film-based solar cell is much lower than that (5.47%) of the anatase TiO₂ microspheres film-based one, which can be mainly ascribed to the much lower J_{sc} as shown in Table 1. On

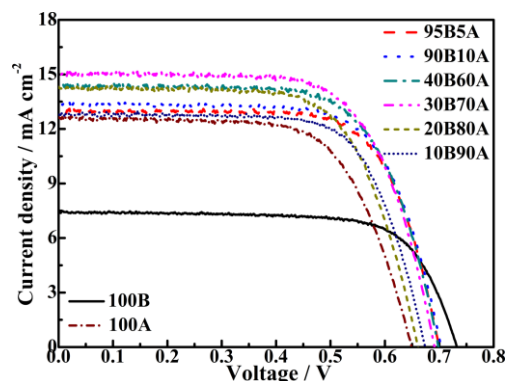


Fig. 5 *J-V* curves of the solar cells fabricated with single or composite electrodes containing different brookite TiO₂ nanocubes and anatase TiO₂ microspheres contents.

Table 1. Photovoltaic performance parameters of the solar cells fabricated with different electrodes

Device ^a	J_{sc} / mA cm ⁻²	V_{oc} / V	FF	η / %
100A	12.63	0.65	0.67	5.47
10B90A	12.78	0.67	0.71	6.09
20B80A	14.31	0.66	0.67	6.38
30B70A	15.12	0.69	0.68	7.09
40B60A	14.38	0.70	0.69	6.90
90B10A	14.36	0.70	0.70	6.61
95B5A	13.00	0.70	0.71	6.47
100B	7.38	0.73	0.73	3.92

^a xByA means the solar cell is made of electrode containing x wt% brookite nanocubes (B) and y wt% anatase microspheres (A).

one hand, it was reported that anatase TiO₂ has a significantly higher dye-loading amount than the brookite TiO₂ even with the same porosity and particle size due to the higher density of dye anchoring sites on the anatase surface.¹⁴⁻¹⁷ On the other hand, the surface area of the present brookite nanocubes is much lower than that of the anatase microspheres as mentioned above. The two aspects could lead to the lower dye-loading amount, which can be validated by the data shown in Fig. 6. As can be seen, the dye-loading amount (4.94×10^{-8} mol cm⁻²) of the brookite TiO₂ nanocubes film electrode is much lower than that (7.44×10^{-8} mol cm⁻²) of the anatase microspheres film, which then cause the brookite TiO₂ nanocubes film-based solar cell (100B) showing much lower J_{sc} and conversion efficiency than the anatase TiO₂ microspheres film-based one (100A). Moreover, it was reported that the poor conductivity of brookite TiO₂ could lead to the significantly lower charge collection efficiency in the brookite solar cell,¹⁶ which also contributes to the lower J_{sc} and efficiency of the corresponding solar cell. Therefore, the low conversion efficiency of the brookite TiO₂ nanocubes film-based solar cell is mainly limited by the dye-loading and the charge collection efficiency. Those limits bring about the difficulty to obtain a satisfactory efficiency from the solar cell that is only fabricated by the brookite nanocubes.¹⁶

Since the plenty of small TiO₂ nanoparticles (with mean diameter of ~15 nm) that exist in the hierarchical structures of the anatase microspheres can play an important role as “nanoglu” to promote the interparticle connection through a dehydration process of the H-bonded network among TiO₂ nanoparticles during the photoanode preparation, and resulting in less charge

recombination and efficient electron transfer in the film electrode, and then higher conversion efficiency.^{21,24-27} Nonetheless, there are many large interspaces still existing among the hierarchical structures of the anatase TiO₂ sea urchin-like microspheres as shown in Fig. 4. Namely, there is a space to further improve the efficiency of the present anatase TiO₂ microspheres film-based solar cell. To take advantage of the higher V_{oc} of the brookite nanocubes and the hierarchical structure of large anatase microspheres, a novel composite electrode containing brookite nanocubes and anatase microspheres is fabricated for further improving the photovoltaic performance of the solar cell. A series of solar cells are fabricated with those composite TiO₂ electrodes, and named as xByA. For instance, 30B70A means the solar cell fabricated with a composite TiO₂ electrode containing 30wt% brookite nanocubes and 70wt% anatase microspheres. Their *J-V* curves and corresponding photovoltaic performance parameters are also listed in Fig. 5 and Table 1. Obviously, all solar cells fabricated with composite TiO₂ electrodes show higher J_{sc} and conversion efficiency compared to the single brookite TiO₂ nanocubes or anatase TiO₂ microspheres film-based one, implying that the introduction of the brookite TiO₂ nanocubes into the anatase TiO₂ microspheres film electrode contribute a significant influence on the performance of the solar cell.

Generally, V_{oc} of a solar cell is determined by the difference between the Fermi level of the TiO₂ electrode and the redox potential of I_3^-/I^- .¹⁴⁻¹⁷ All solar cells fabricated with composite TiO₂ electrode display a higher V_{oc} than the single anatase TiO₂ microspheres film-based one, and the V_{oc} is gradually enhanced from 0.65 V to 0.70 V with enhancing the brookite nanocubes content from 0 to 40wt%, and then maintains unchanged upon further enhancing the brookite content to 95wt%. Therefore, it can be concluded that introducing the brookite TiO₂ nanocubes into the anatase TiO₂ microspheres film can enhance the Fermi level of the composite TiO₂ electrode, and then causing the increasing V_{oc} value upon enhancing the brookite content. It is consistent with the above conclusion that the brookite nanocubes have a higher CB level than the anatase microspheres due to their same elementary composition contributing an identical VB level.⁵⁻⁷ Similarly, introducing the brookite TiO₂ nanocubes into the anatase TiO₂ microspheres film electrode also leads to the enhancement in the J_{sc} and conversion efficiency (η) of the solar cells as shown in Table 1. Upon enhancing the brookite nanocubes content from 0 to 30wt%, the J_{sc} value of the solar cell can be gradually increased from 12.63 to 15.12 mA cm⁻², and then decreases to 13.00 mA cm⁻² with further enhancing the brookite nanocubes content to 95wt%. Namely, the 30B70A solar cell fabricated with the composite TiO₂ electrode containing 30wt% brookite and 70wt% anatase exhibits the highest J_{sc} value among those solar cells tested, which achieves the maximum efficiency of 7.09%, improved by 81% or 30% as compared to the single brookite TiO₂ nanocubes (100B) or anatase TiO₂ microspheres (100A) film-based solar cell, respectively.

The above changing trend in photocurrent and efficiency is mainly related to the dye-loading amount. Fig. 6 displays the effect of the brookite TiO₂ nanocube mass ratio in the anatase TiO₂ microsphere film electrode on the dye-loading amount of the composite TiO₂ electrodes. As can be seen, the dye-loading amount shows an increasing trend upon enhancing the brookite

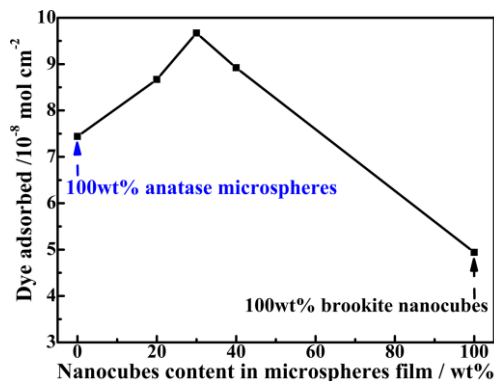


Fig. 6 Effect of the brookite TiO_2 nanocube content in the anatase microspheres TiO_2 film on the dye-loading amount of the various electrodes.

content from 0 to 30wt%, and then decrease with further enhancing the brookite content to 100wt%. Since the brookite nanocubes have much lower surface area and dye-anchoring site density than the anatase microsphere,¹⁴⁻¹⁷ which could lead to the decrease in the total specific surface area and dye-loading amount of those composite TiO_2 electrodes with enhancing the brookite content. However, the decrease in the dye-loading amount is observed only when the brookite content is $\geq 30\text{wt}\%$ (Fig. 6), and the dye-loading amount shows an increasing trend with enhancing the brookite content from 0 to 30wt%. This phenomenon might imply that a suitable quantity of brookite nanocubes can be embedded into the interspaces of the anatase microspheres to form intimate contacts between the anatase and brookite TiO_2 , which is a benefit to enhance the TiO_2 content in the film with a similar thickness, then causing the increased total surface area and the dye-loading amount in the film electrode when the brookite nanocubes content is $\leq 30\text{wt}\%$.

Once the brookite content exceeds 30wt%, the obvious decrease of the anatase microsphere content in the composite electrode would lead to the reduction of total surface area, and then the reduced dye-loading amount as shown in Fig. 6, which further causing the significant decreases in both J_{sc} and conversion efficiency. Moreover, the poor conductivity of the brookite would also lead to the gradual decrease of the J_{sc} and efficiency upon enhancing the brookite content in the composite film electrode.¹⁶ Nevertheless, the 95B5A solar cell still shows a 6.47% efficiency with $J_{\text{sc}}=13.00 \text{ mA cm}^{-2}$ even the brookite nanocubes content is up to 95wt%. It is higher than that of the single brookite TiO_2 nanocubes (100B) or anatase TiO_2 microsphere (100A) film-based one, indicating that introducing the brookite nanocubes into the anatase microsphere film electrode can not only enhance the photovoltage and photocurrent, but also improve the photovoltaic performance of the solar cell. Therefore, it can be concluded that the specific features such as large sphere diameter and specific surface area, urchin-like hierarchical structure are beneficial for some brookite TiO_2 nanocubes embedded into the interspaces of the microspheres to form intimate contacts between the anatase and brookite TiO_2 . It can significantly enhance the charge separation and then the photoelectric conversion of the solar cells, which will be further discussed below.

3.3 Electrochemical impedance spectra analyses

To further understand the effect of the introduction of the brookite nanocubes in the anatase microspheres film electrode on the performance of the solar cell, the electrochemical impedance spectra (EIS) of the solar cells fabricated with the single anatase microspheres (100A), the brookite nanocubes (100B), and their composite film electrode (30B70A) are obtained at the open-circuit voltage and AM1.5 illumination. Fig. 7a and b show their Nyquist and Bode plots, and the corresponding fitted photoelectrochemical parameters according to the equivalent circuit model inserted in Fig. 7a are listed in Table 2. Usually, Nyquist diagram features three semicircles that can be attributed to the Nernst diffusion within the electrolyte, the electron transfer at the oxide/electrolyte interfaces, and the redox reaction at the Pt counter electrode in the order of increasing frequency.²⁸

In the Nyquist plots (Fig. 7a) of the three solar cells, only two obvious semicircles can be detected since the semicircle attributed to the Nernst diffusion within the electrolyte is featureless due to the relatively fast diffusion of the present liquid electrolyte in the porous film electrodes.²⁹ The semicircle in high frequency region can be ascribed to the charge transfer resistance (R_1) at the redox electrolyte/Pt counter electrode interfaces; and

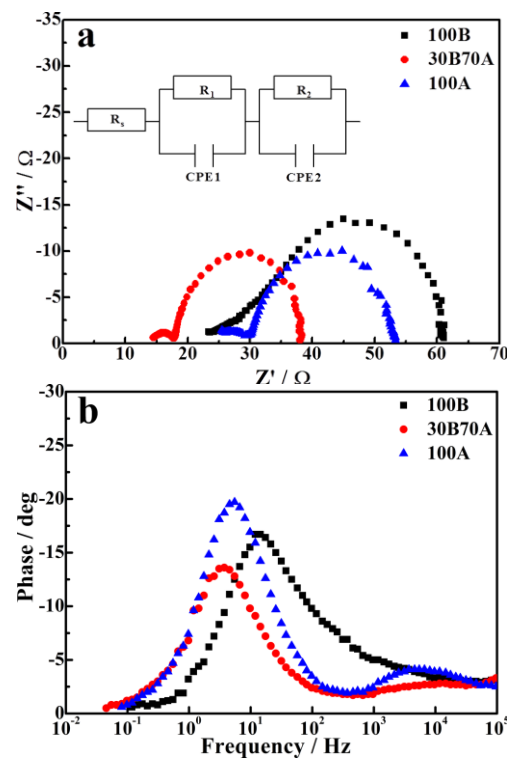


Fig. 7 EIS spectra of the solar cells fabricated with the single TiO_2 or composite electrode containing 30wt% brookite nanocubes and 70wt% anatase microspheres. Nyquist plots (a); Bode plots (b).

Table 2 Electrochemical performance parameters of the solar cells fabricated with different electrodes

Device	$R_s / \Omega \text{ cm}^2$	$R_1 / \Omega \text{ cm}^2$	$R_2 / \Omega \text{ cm}^2$	f / Hz	τ_n / ms
100A	25.06	4.47	23.8	5.5	29.0
30B70A	14.46	3.36	20.2	3.7	43.0
100B	23.35	3.71	33.9	14.4	11.1

the semicircle in middle frequency region is related to the resistance (R_2) of the accumulation/transport of the injected electrons within TiO_2 film and the charge transfer across either the TiO_2 /dye/redox electrolyte or the FTO/ TiO_2 interfaces; R_s (the intercept on the real axis at the highest frequency of Nyquist plot) represents the serial resistance which is determined by the sheet resistance between TiO_2 substrate and the conductive layers of FTO glass. As can be seen from Table 2, the R_s value of the 100B, 30B70A and 100A solar cell is 23.35, 14.46, and 25.06 Ω , respectively. It seems that the solar cell fabricated with the composite TiO_2 electrode containing 30wt% brookite nanocubes appears a significant decrease in the serial resistance, which is related to the contact resistance between the TiO_2 film and the FTO conductive layer.^{30,31} As mentioned above, the small brookite TiO_2 nanocubes can fill into the interspaces of the large sea urchin-like TiO_2 hierarchical microspheres, which resulting in the increase of the contact area between the TiO_2 film and the FTO substrate, and then the lower serial resistance (R_s) for the solar cell fabricated with the composite electrode as compared to the single anatase microsphere or the brookite nanocubes electrode since all cells have the same FTO-substrate.

Similarly, introducing 30wt% brookite nanocubes into anatase microspheres electrode also leads to the lower electron transfer resistance (R_2) at the TiO_2 /electrolyte interfaces as shown in Table 2, indicating the charge transfer process at the composite TiO_2 film/electrolyte interfaces is more efficient than that at the single anatase microsphere or brookite nanocubes film/electrolyte interfaces. It would be beneficial for enhancing the electron injection efficiency in the composite electrode. Moreover, the higher CB level of the brookite than anatase TiO_2 is also a benefit of the electron injections to FTO substrate, which produce a stronger driving force for the electron injection in the solar cell fabricated with the composite film. The above two aspects would lead to the R_2 decrease of the composite TiO_2 -based solar cell, which further leads to the increased photocurrent and conversion efficiency as mentioned above.

A low R_2 is favourable for the electron transport through a longer distance with less diffusive hindrance to some extent, and thus probably resulting in the reduced electron recombination and the longer lifetime.²⁹ This conjecture can be validated by the data shown in Table 2. The lifetime (τ_n) of injected electrons in the solar cell can be determined by the position of the low frequency peak in Bode plots (Fig.7b) through the equation that $\tau_n=1/(2\pi f)$ where f means the frequency of superimposed AC voltage.²⁸ As can be seen from Table 2, the solar cell fabricated with composite electrode containing 30wt% brookite nanocubes shows the longest lifetime (43 ms) among those solar cells tested, enhanced by 3.87 and 1.48 times as compared to the single brookite TiO_2 nanocubes or the anatase TiO_2 microspheres film-based one, respectively. Namely, introducing the brookite nanocubes can significantly prolong the electron lifetime, which can be ascribed to the poor conductivity of brookite compared to anatase. It means that the solar cell fabricated with composite electrode has a reduced charge recombination and longer electron lifetime, which then resulting in the higher V_{oc} than the anatase one.¹⁶

3.4 Open-circuit voltage decay curve analyses

The main information on the interfacial recombination processes

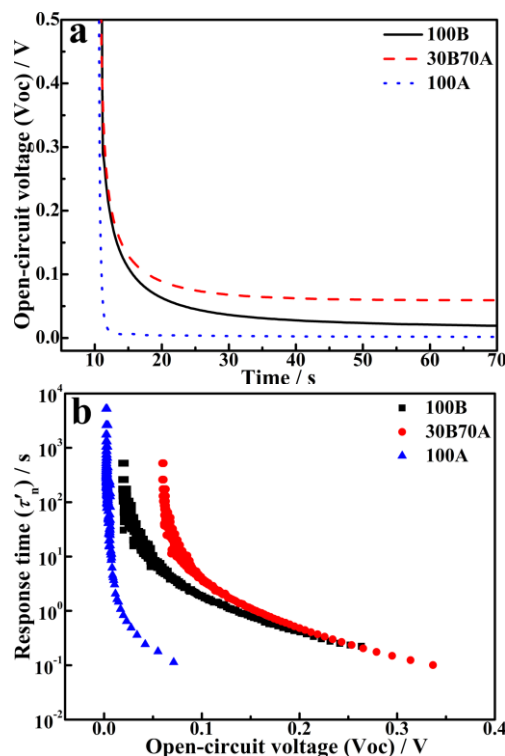


Fig. 8 Open-circuit voltage decay (OCVD) curves (a) and corresponding τ_n' - V_{oc} curves (b) of the solar cells fabricated with the single TiO_2 or composite electrode containing 30wt% brookite nanocubes and 70wt% anatase microspheres.

between the photoinjected electrons in the TiO_2 electrode and electrolyte under the dark state can be obtained from the open-circuit voltage decay (OCVD) curve.³²⁻³⁴ The difference of cell's open-circuit voltage (V_{oc}) can change the electron lifetime (τ_n') due to the shift of semiconductors Fermi level. Hence, to estimate the shapes of $\tau_n' \sim V_{oc}$ relation curves of the solar cell, we can have a qualitative understanding on the effects of the electron traps on the recombination reaction. The electron lifetime (τ_n') can be derived from the OCVD measurements according to Eq. 1:

$$\tau_n' = -\frac{k_B T}{e} \left(\frac{dV_{oc}}{dt} \right)^{-1} \quad (1)$$

where k_B is the Boltzmann constant, T is the temperature, e is the electron charge.

Fig. 8a shows the open-circuit voltage decay (OCVD) curves of the solar cells fabricated with the single anatase microspheres (100A), the brookite nanocubes (100B), and their composite film electrode (30B70A) under open-circuit and dark conditions. Under the present open-circuit and dark conditions, the electron transport resistance in the TiO_2 film has no effect on the OCVD measurements because of there is no current flow through the cell. Once the light was shut off, the V_{oc} of the single anatase microspheres TiO_2 -based solar cell decays near to 0 only after 15 s decay time, while the solar cells fabricated with the single brookite nanocubes and the composite film electrode still maintain ~ 0.05 and 0.1 V even after 60 s, respectively. It implies that introducing 30wt% brookite nanocubes in the composite film electrode can lead to a less charge recombination and longer electron lifetime as compared to the single anatase TiO_2 microspheres film-based solar cell. Fig. 8b shows the electron lifetime (τ_n') $\sim V_{oc}$ relation curves of the above solar cells derived

from Fig. 8a. As can be seen, the τ_n' value shows an exponential dependence at the V_{oc} , and the 30B70A solar cell fabricated with the composite TiO₂ electrode has a much longer electron lifetime than that of the single brookite nanocubes and anatase microspheres film-based one.

This phenomenon can be understandable according to Zaban's suggestion.³⁵ In Zaban's model, the electron lifetime is mainly affected by the surface state traps in the TiO₂ film explained by the shape of $\tau_n' \sim V_{oc}$ curve qualitatively.^{32,35} Typically, $\tau_n' \sim V_{oc}$ relation curves can be divided into three parts in which the lifetime is dominated by different factors: a constant lifetime at high voltage related to free electrons, an exponential dependence at medium potential due to the internal trapping and detrapping, and an inverted parabola at low voltage corresponding to the reciprocal of the density of levels of acceptor electrolyte species. The linear dependence of electron lifetime on V_{oc} turned into a curved one because the charge transfer process is mainly governed by the distribution of surface traps. Obviously, the electron lifetime increases significantly at medium and low voltage regions when the brookite TiO₂ nanocubes are introduced in the anatase TiO₂ microspheres film electrode. Moreover, the presence of those brookite TiO₂ nanocubes with a higher CB in the interspaces of those anatase TiO₂ microspheres film can also block the back flow of the injected electrons, which can be inferred from the higher remaining voltage in the OCVD curves (Fig. 8a), and then decreases the charge recombination.

On the bases of the above results and discussion, the present brookite TiO₂ nanocubes with small size and high phase purity can be mixed with the anatase TiO₂ microspheres to obviously improve the photovoltaic performance of the solar cell due to the following reasons. 1) Although the brookite TiO₂ nanocubes have much lower surface area and less dye anchoring sites than the anatase TiO₂ microsphere, the dye-loading amount still can be enhanced when the brookite TiO₂ nanocubes content is $\leq 30\text{wt}\%$ since those brookite TiO₂ nanocubes can fill into the interspaces of the sea urchin-like hierarchical structures of the anatase TiO₂ microspheres, and cooperate with the anatase microspheres film to load more dye molecules, which leads to the solar cell fabricated with the composite TiO₂ electrode showing significantly enhanced J_{sc} compared to the single anatase TiO₂ microsphere film-based cell; 2) The higher CB level of the brookite than anatase TiO₂ can not only promote the electron injections from the brookite to the anatase, but also retard the charge recombination, and then causing a longer electron lifetime and higher photovoltage as compared to the single anatase TiO₂ microspheres film-based one. Nevertheless, the poor dye adsorption capacity and lower surface area of the brookite nanocubes compared to the anatase microspheres limits the quantity of the photoexcited electrons when the brookite nanocubes content in the composite electrode beyond 30wt% as described above, which leads to the reduced dye-loading amount, shorter electron lifetime and lower photocurrent. Consequently, the solar cell fabricated with the composite electrode containing 30wt% brookite nanocubes gives a conversion efficiency of 7.09%, with 81% or 30% improvement in the efficiency as compared to the single brookite TiO₂ nanocubes or anatase TiO₂ microspheres film-based solar cell. Namely, introducing the brookite TiO₂ nanocubes into the anatase TiO₂ microsphere film

electrode with suitable amount and particle size can not only reduce the charge recombination, but also enhance the electron injection efficiency and prolong the electron lifetime. All these could lead to the higher voltage and photocurrent, and then causing the improved photovoltaic performance of the anatase TiO₂ film-based solar cell.

4 Conclusion

In summary, thermally stable brookite TiO₂ quasi nanocubes with high phase purity and a mean particle size of ~ 50 nm are synthesized through a hydrothermal method, and anatase TiO₂ microspheres with ~ 3 μm diameter and sea urchin-like hierarchical structure containing secondary TiO₂ nanoribbons and nanoparticles (average particle size of ~ 15 nm) are synthesized through a one-step solvothermal method. To efficiently exploit the advantages of those TiO₂ particles with different crystal phases and morphology, a novel composite electrode containing the brookite TiO₂ nanocubes and anatase TiO₂ sea urchin-like microspheres is fabricated for improving the photovoltaic performance of the TiO₂-based dye-sensitized solar cells. It is found that the distinctive structure features such as large sphere diameter and specific surface area, urchin-like hierarchical structure of the anatase TiO₂ microspheres are beneficial for the brookite nanocubes embedded into the interspaces of the microspheres to form intimate contacts between the anatase and brookite TiO₂, which leads to the enhanced photovoltage and photocurrent, and then the improved photovoltaic performance of the solar cell. As a result, the solar cell fabricated with the composite electrode containing 30wt% brookite nanocubes gives a conversion efficiency of 7.09%, with 81% or 30% improvement in the efficiency as compared to the single brookite TiO₂ nanocubes or anatase TiO₂ microspheres film-based solar cell. Namely, introducing the brookite TiO₂ nanocubes into the anatase TiO₂ microsphere electrode with suitable amount and particle size can not only reduce the charge recombination, but also prolong the electron lifetime and enhance the electron injection efficiency. All these could lead to the higher voltage and photocurrent, and then causing the improved photovoltaic performance of the anatase TiO₂ film-based solar cell. The work presented here suggests a new route to take advantage of TiO₂ particles with different crystal phases and morphology to efficiently improve the photovoltaic performance of the anatase TiO₂-based solar cells.

Acknowledgements

This work was supported by the National Natural Science Foundation of China (21271146, 20973128, and 20871096), Program for New Century Excellent Talents in University of China (NCET-07-0637), the Funds for Creative Research Groups of Hubei Province (2014CFA007), and Fundamental Research Funds for the Central Universities (2042014kf0228).

Notes and references

College of Chemistry and Molecular Science, Wuhan University, Wuhan 430072, P. R. China. Fax: 86 27 6875 2237; Tel: 86 27 6875 2237; E-mail: typeng@whu.edu.cn (T. Peng)

Keywords: anatase microsphere • brookite nanocube • composite film electrode • dye-sensitized solar cell • photoelectrochemical property

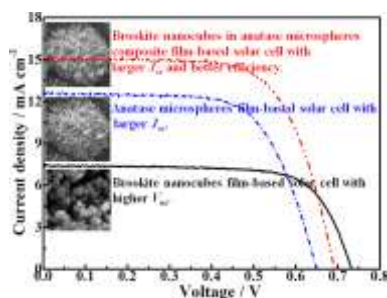
35 J. Bisquert, A. Zaban, M. Greenshtein and I. Mora-Sero, *J. Am. Chem. Soc.*, 2004, **126**, 13550–13559.

- 1 B. O'Regan and M. Grätzel, *Nature*, 1991, **353**, 737–740.
- 2 M. M. Foroushani, H. Dehghani and N. S. Vanani, *Electrochim. Acta*, 2013, **92**, 315–322.
- 3 A. Yella, H. W. Lee, H. N. Tsao, C. Y. Yi, A. K. Chandiran, M. K. Nazeeruddin, E. W. G. Diau, C. Y. Yeh, S. M. Zakeeruddin and M. Grätzel, *Science*, 2011, **334**, 629–634.
- 4 H. P. Zhou, Q. Chen, G. Li, S. Luo, T. Song, H. S. Duan, Z. Hong, J. B. You, Y. S. Liu and Y. Yang, *Science*, 2014, **345**, 542–546.
- 5 S. D. Mo and W. Y. Ching, *Phys. Rev. B*, 1995, **51**, 13023–13032.
- 6 M. M. Rodriguez, X. H. Peng, L. J. Liu, Y. Li and J. M. Andino, *J. Phys. Chem. C*, 2012, **116**, 19755–19764.
- 7 B. Ohtani, J. Handa, S. Nishimoto and T. Kagiya, *Chem. Phys. Lett.*, 1985, **120**, 292–294.
- 8 Y. L. Liao, W. X. Que, Q. Y. Jia, Y. C. He, J. Zhang and P. Zhong, *J. Mater. Chem.*, 2012, **22**, 7937–7944.
- 9 T. Kandiel, L. Robben, A. Alkaim and D. Bahnemann, *Photoch. Photobiol. Sci.*, 2013, **12**, 602–609.
- 10 M. Ni, M. K. H. Leung, D. Y. C. Leung and K. Sumathy, *Renew. Sustain. Energy Rev.*, 2007, **11**, 401–425.
- 11 W. B. Hu, L. P. Li, G. S. Li, C. L. Tang and L. Sun, *Cryst. Growth Des.*, 2009, **9**, 3676–3682.
- 12 H. F. Lin, L. P. Li, M. L. Zhao, X. S. Huang, X. M. Chen, G. S. Li and R. C. Yu, *J. Am. Chem. Soc.*, 2012, **134**, 8328–8331.
- 13 S. Ardizzone, C. L. Bianchi, G. Cappelletti, S. Gialanella, C. Pirola and V. Ragaina, *J. Phys. Chem. C*, 2007, **111**, 13222–13231.
- 14 C. Magne, S. Cassaignon, G. Lancel and T. Pauporté, *ChemPhysChem*, 2011, **12**, 2461–2467.
- 15 C. Magne, F. Dufour, F. Labat, G. Lancel, O. Durupthy, S. Cassaignon and T. Pauporté, *J. Photochem. Photobiol. Chem.*, 2012, **232**, 22–31.
- 16 Y. Kusumawati, M. Hosni, M. A. Martoprawiro, S. Cassaignon and T. Pauporté, *J. Phys. Chem. C*, 2014, **118**, 23459–23467.
- 17 M. Koelsch, S. Cassaignon, T. T. Minh, J. F. Guillemoles and J. P. Jolivet, *Thin Solid Films*, 2004, **451/452**, 86–92.
- 18 K. J. Jiang, T. Kitamura, H. Yin, S. Ito and S. Yanagida, *Chem. Lett.*, 2002, **31(9)** 872–873.
- 19 K. Li, J. L. Xu, W. Y. Shi, Y. B. Wang and T. Y. Peng, *J. Mater. Chem. A*, 2014, **2** 1886–1896.
- 20 J. L. Xu, K. Li, W. Y. Shi, R. J. Li and T. Y. Peng, *J. Power Sources*, 2014, **260**, 233–242.
- 21 K. Fan, T. Y. Peng, J. N. Chen, X. H. Zhang and R. J. Li, *J. Power Sources*, 2013, **222**, 38–44.
- 22 J. G. Li, C. C. Tang, D. Li, H. Haneda and T. Ishigaki, *J. Am. Ceram. Soc.*, 2001, **87**, 1358–1361.
- 23 Y. Li, W. Lee, D. K. Lee, K. Kim, N. G. Park and M. J. Ko, *Appl. Phys. Lett.*, 2011, **98**, 103301.
- 24 X. Li, H. Lin, J. B. Li, N. Wang, C. F. Lin and L. Z. Zhang, *J. Photochem. Photobiol. A*, 2008, **195**, 247–253.
- 25 T. Miyasaka, M. Ikegami and Y. Kijitori, *J. Electrochem. Soc.*, 2007, **154**, A455–A461.
- 26 T. Miyasaka, Y. Kijitori and M. Ikegami, *Electrochem.*, 2007, **75**, 2–12.
- 27 K. Fan, C. Q. Gong, T. Y. Peng, J. N. Chen and J. B. Xia, *Nanoscale*, 2011, **3**, 3900–3906.
- 28 D. Zhao, T. Y. Peng, L. L. Lu, P. Cai, P. Jiang and Z. Q. Bian, *J. Phys. Chem. C*, 2008, **112**, 8486–8494.
- 29 Y. Z. Zheng, X. Tao, L. X. Wang, H. Xu, Q. Hou, W. L. Zhou and J. F. Chen, *Chem. Mater.*, 2009, **22**, 928–934.
- 30 T. Hoshikawa, M. Yamada, R. Kikuchi and K. Eguchi, *K. J. Electrochem. Soc.*, 2005, **152**, E68–E73.
- 31 T. N. Murakami, S. Ito, Q. Wang, M. K. Nazeeruddin, T. Bessho, I. Cesar, P. Liska, R. Humphry-Baker, P. Comte, P. Pechy and M. Grätzel, *M. J. Electrochem. Soc.*, 2006, **153**, A2255–A2261.
- 32 K. Fan, W. Zhang, T. Y. Peng, J. N. Chen and F. Yang, *J. Phys. Chem. C*, 2011, **115**, 17213–17219.
- 33 T. Y. Peng, K. Fan, D. Zhao and J. N. Chen, *J. Phys. Chem. C*, 2010, **114**, 22346–22351.
- 34 R. Kern, R. Sastrawan, J. Ferber, R. Stangl and J. Luther, *Electrochim. Acta*, 2002, **47**, 4213–4225.

Entry for the Table of Contents

Composite electrode of TiO₂ particles with different crystal phases and morphology to significantly improve the performance of dye-sensitized solar cells

Jinglei Xu, Jingpeng Jin, Zihao Ying, Wenye Shi, and Tianyou Peng*



Novel composite TiO₂ electrode containing brookite nanocubes and anatase sea urchin-like microspheres is fabricated for improving the dye-sensitized solar cell's performance.